



Assessment of Liquid Crystal Template Deposited Porous Nickel as a Supercapacitor Electrode Material

V. Ganesh,^a V. Lakshminarayanan,^{a,*} and S. Pitchumani^b

^aRaman Research Institute, Bangalore-560080, India

^bCentral Electrochemical Research Institute, Karaikudi-630006, India

The high surface area porous nickel, obtained by template electrodeposition using a hexagonal liquid crystalline phase medium as a template was evaluated as a potential material for electrochemical capacitors using cyclic voltammetry (CV) and electrochemical impedance spectroscopy (EIS) studies in 6 M KOH. A single electrode double layer capacitance of 1.4 F/cm² (at 2 mV/s scan rate) was obtained using CV, which corresponds to a specific capacitance of 473 F/g. EIS studies show the typical behavior of a porous electrode and the data were analyzed in terms of complex capacitance and complex power from which the relaxation time constant (τ_0) has been determined. Nickel oxide electrode, obtained by the electrochemical oxidation of porous Ni, shows a double layer capacitance value of 171 mF/cm², which corresponds to a specific capacitance of 57 F/g. The relaxation time constants for the template deposited porous nickel and nickel oxide were determined to be 1.35 s and 33 ms, respectively. The values of double layer capacitance and specific capacitance of the porous nickel with fast response time are the highest values reported for nickel in the literature so far.

© 2005 The Electrochemical Society. [DOI: 10.1149/1.1911931] All rights reserved.

Manuscript submitted November 24, 2004; revised manuscript received March 4, 2005. Available electronically April 21, 2005.

Recently, we have reported the preparation of high surface area porous nickel using liquid crystal template electrodeposition method.¹ It was shown by scanning tunneling microscopy (STM) and scanning electron microscopy (SEM) studies that the template deposited Ni surface exhibits porous structure with nickel nanoparticles being distributed in between as well as within the pores. We also evaluated the utility of this porous nickel as a high surface area hydrogen evolution catalyst and indicated the potential application of this material in electrochemical capacitors (ECs). These capacitors are often known by various names such as supercapacitors, ultracapacitors, power capacitors, gold capacitors, power cache, electrochemical double layer capacitors (EDLCs), etc. and generally fall under the category of energy storage devices.² Recently, much research work has focused on ECs due to their application in high power devices such as lasers, electric vehicles (for acceleration) and also in variety of other energy storage applications.³⁻⁵ There are two modes of energy storage mechanism operative in ECs, those based on the double layer capacitance arising from the separation of charges at the electrode/electrolyte interface and those based on the pseudocapacitance arising from faradaic reactions occurring at or near the solid electrode surface due to the presence of electroactive materials. The utility of EDLCs is limited by the maximum capacitance range (10 - 40 μ F/cm²),⁶ electrochemical stability of the electrolyte, and the utilization of electrode surface area due to the presence of non-wettable micropores.⁷ The well-known electrochemical double layer capacitors are normally based on the high surface area carbon materials such as activated carbon, carbon fiber cloth and carbon aero gels/foams having high specific capacitance values.⁸ However, there are some limitations on the performance of these capacitors due to the nonwettability of the pores by the electrolyte and also from the inherently associated high internal resistance.⁹

On the other hand, transition metal oxides like ruthenium oxide (RuO₂) and iridium oxide (IrO₂) exhibit faradaic pseudocapacitance behavior with single electrode capacitance values between 720 and 760 F/g.^{10,11} Despite the impressive capacitance values and high reversibility obtained due to the faradaic redox reactions within these electroactive materials, the high cost of ruthenium and iridium has restricted its applications. In general, the ability to deliver the high power density of supercapacitors is decided by the reversibility of the electrode/electrolyte interface.^{12,13}

There are several reports on alternative electrode materials such as nickel oxide,¹⁴⁻¹⁷ cobalt oxide,¹⁸ and manganese oxide,¹⁹ which are inexpensive and exhibit pseudocapacitive behavior that are being

used as supercapacitors. Among them, NiO is attractive in view of its well-defined electrochemical redox activity and the possibility of enhanced performance through different preparative methods. The results of NiO were based on the preparation of nickel hydroxide either from sol-gel technique¹⁴ or from electrodeposition process^{15,16} followed by heating in air to form nickel oxide. The specific capacitance values varying from 240 to 260 F/g were reported. In addition to the higher specific capacitance values when compared to the carbon materials, the ability to produce thin films of NiO makes it an attractive material for high-power devices. Recently, Nelson and Owen reported the fabrication of a supercapacitor/battery hybrid using a mesoporous Ni/Ni(OH)₂ positive electrode and a mesoporous Pd negative electrode. This system was able to deliver 166 mA h/g of Ni electrode in 50 ms at a mean discharge voltage of 1.18 V using 6 M KOH. These values translate into an energy density of 706 kJ/kg and a power density of 14.1 MW/kg.²⁰

The high surface area porous nickel reported previously¹ showed a roughness factor value as high as 3620, making it a potential candidate for supercapacitor applications. In this paper, we report the performance characteristics of such a high surface area porous nickel and its corresponding NiO electrodes as EC electrode materials. These electrodes will be used in a cell assembly presently under development, and the results will be reported elsewhere in a later paper. The electrochemical characteristics of these electrode materials have been evaluated using cyclic voltammetry (CV) and electrochemical impedance spectroscopy (EIS) in an aqueous electrolyte of 6 M KOH. The EIS data were analyzed in terms of complex power and complex capacitance from which the relaxation time constant (τ_0) had been determined.

Experimental

High surface area porous nickel was prepared from a new hexagonal liquid crystalline phase consisting of 42 wt % Triton X-100, 5 wt % PAA, and 53 wt % water in which the water phase was replaced by nickel sulfamate bath as reported in our previous work.¹ After deposition, the roughness factor of the porous nickel electrode was determined using CV by scanning the potential from -1.2 to -0.2 V vs. SCE in 0.5 M NaOH solution and measuring the charge under the anodic oxidation peak.¹

Electrochemical characterization of porous nickel and its corresponding nickel oxide as electrochemical capacitor electrode materials was carried out in an all glass three-electrode system. A platinum foil of large surface area was used as a counter electrode and a saturated calomel electrode (SCE) as a reference electrode. CV was performed in the double layer region of potential from -1.1 to -0.9 V vs. SCE in 6 M KOH solution at various potential scan rates.

* Electrochemical Society Active Member.

^z E-mail: narayan@rri.res.in

Before the beginning of the experiments the electrode was maintained at a potential of -1.6 V vs. SCE for 600s in the alkaline solution. This process reduces the surface oxides and cathodically cleans the surface by the evolution of hydrogen gas. This is followed by keeping the electrode at a potential of -1.02 V vs. SCE that oxidizes any metal hydrides on the surface.²¹ Finally, the porous nickel electrode was scanned in the double layer region to determine the capacitance.

Electrochemical oxidation of porous nickel to its corresponding nickel oxide has been carried out by potential scanning at the nickel oxide region.^{22,23} First, the potential was cycled between -0.1 and $+0.5$ V vs. SCE in the alkaline solution for more than 25 cycles at various scan rates, where the NiO formation and its stripping take place. The capacitance was then determined by scanning the oxidized nickel oxide electrode in the potential range from -0.1 to $+0.2$ V vs. SCE at different scan rates and measuring the integrated charge. The potential scan rates for voltammetric experiments were varied from 2 to 500 mV/s.

EIS was performed in 6 M KOH aqueous solution by applying a sinusoidal signal of 5 mV peak-to-peak amplitude at a frequency range from 100 mHz to 100 kHz. All of the electrochemical measurements were carried out using an EG&G electrochemical impedance analyzer (model 6310) which can be operated both in dc and ac modes and interfaced to a PC through GPIB card (National instruments). The equivalent circuit fitting has been carried out using Zsimpwin software (EG&G) developed on the basis of Boukamp's model. All of the chemical reagents used were AnalaR (AR) grade. Millipore water having a resistivity of 18 M Ω cm was used in all the experiments performed at a room temperature of 25°C.

Results and Discussion

CV measurement of specific capacitance in the double layer region.—For the porous nickel electrode.—CV is an important technique for evaluating the capacitive behavior of any material. A perfect rectangular shaped voltammogram with a large current separation and symmetric in both cathodic and anodic directions are the indicators of an ideal capacitor. Figure 1a shows the CVs of porous nickel electrode scanned in the double layer region of -1.1 to -0.9 V vs. SCE at various scan rates in 6 M KOH aqueous solution. It can be seen that the CVs show no visible peak formation but has a large current separation between forward and reverse scans. The CVs possess almost rectangular shape, especially at higher scan rates indicating capacitive behavior. The capacitance values are determined by measuring the integrated charge from the CV. It is felt that there may be a substantial pseudocapacitance contribution to the overall measured capacitance of the porous nickel electrode.

Table I shows the double layer capacitance and specific capacitance values for porous nickel at different scan rates. For comparison, the capacitance values of smooth nickel electrode were also given. A single electrode capacitance of 1.4 F/cm² obtained at 2 mV/s scan rate corresponds to a specific capacitance value of 473 F/g. The fact that CVs show good rectangular features and are symmetrical at higher scan rates (even at 500 mV/s) indicates that it has good electrochemical activity and high power density. Figure 2a shows the variation of specific capacitance with scan rate and Fig. 2b shows the variation of the current density measured from CV with scan rate. The specific capacitance increases exponentially with decreasing scan rate. Similar behavior is reported in the literature for various electrode materials.²⁴⁻²⁷ In the case of RuO₂ supercapacitor,²⁶ this is attributed to increasing ionic resistance inside the pores leading to a decrease in capacitance. A similar effect is believed to operate in the present porous Ni system where the surface reaction due to nickel hydride formation contributes to large pseudocapacitance. The formation of nickel hydride in alkaline media is well established in the literature.²⁸⁻³⁰ The contribution of substantial pseudocapacitance is also suggested by the scan rate dependence of the potential when plotted against I/v (v is scan rate). The high power characteristics of the porous nickel can be inferred from Fig. 2b, which shows almost linear variation of CV current density

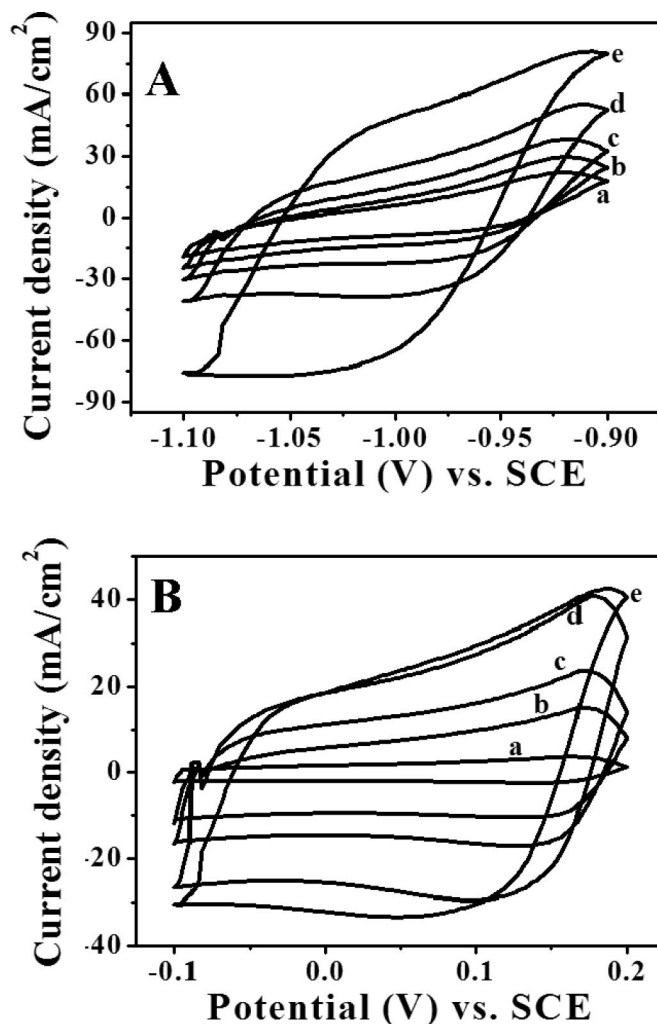


Figure 1. (A) CVs of template deposited porous nickel in 6 M KOH solution at scan rates of (a) 25, (b) 50, (c) 100, (d) 200, and (e) 500 mV/s. (B) CVs of nickel oxide electrode obtained by electrochemical oxidation of porous nickel in 6 M KOH aqueous solution at scan rates of (a) 25, (b) 50, (c) 100, (d) 200, and (e) 500 mV/s.

with the scan rate. The incomplete formation and subsequent oxidation of metal hydride at higher scan rates can lead to lowering of the measured capacitance with the increasing scan rate as observed in Fig. 2a. It is also evident that the porous nickel electrode exhibits good high power characteristic as seen from Fig. 2b, which shows an almost linear variation of current density with the scan rate.

For nickel oxide (NiO) electrode.—Figure 1b shows the CVs of nickel oxide electrode at various scan rates in 6 M KOH aqueous solution. It is evident that the nickel oxide electrode shows a typical capacitive behavior with no redox peaks formation. Table I shows the capacitance and specific capacitance values for nickel oxide electrode, obtained by electrochemical oxidation of the porous nickel at different scan rates. A very high single electrode capacitance value of 171 mF/cm², which translates into a specific capacitance of 57 F/g has been measured at a scan rate of 50 mV/s. A specific capacitance value of 260 F/g was earlier reported in the literature for nickel oxide electrode.²³ In that case, the capacitive behavior was due to the nickel oxide phase being formed by heating the electrodeposited Ni(OH)₂ to a temperature above 250°C. However, the specific capacitance value decreased to 146 F/g when heated to a temperature above 300°C.²³ These high capacitance values were attributed to the change in surface area and

Table I. The capacitance (C) and specific capacitance (C_s) values of porous nickel and its corresponding nickel oxide electrodes obtained from CV. For comparison smooth nickel values are also given.

Scan rate (mV/s)	C ($\mu\text{F}/\text{cm}^2$) (Smooth Ni)	C (mF/cm^2) (Porous Ni)	C_s (F/g) (Porous Ni)	C (mF/cm^2) (NiO)	C_s (F/g) (NiO)
2	3.70	1418	473	74	24.67
5	2.45	678	226	86	28.67
10	1.80	437	146	82	27.33
25	1.14	297	99	80	26.67
50	1.08	228	76	171	57
100	0.75	187	62	142	47.33
200	0.50	158	52	125	41.67
500	0.32	114	38	57	19

the nonstoichiometric nature of NiO that is formed. In the present study, we employed the direct electrochemical oxidation of porous nickel to nickel oxide through nickel hydroxide formation by simply scanning at a potential range where NiO formation and subsequent stripping take place. The lower values of capacitance obtained by the electrochemical oxidation method in our system can be attributed to incomplete conversion of nickel to nickel oxide within the pores. The potential window in which the capacitance is measured is

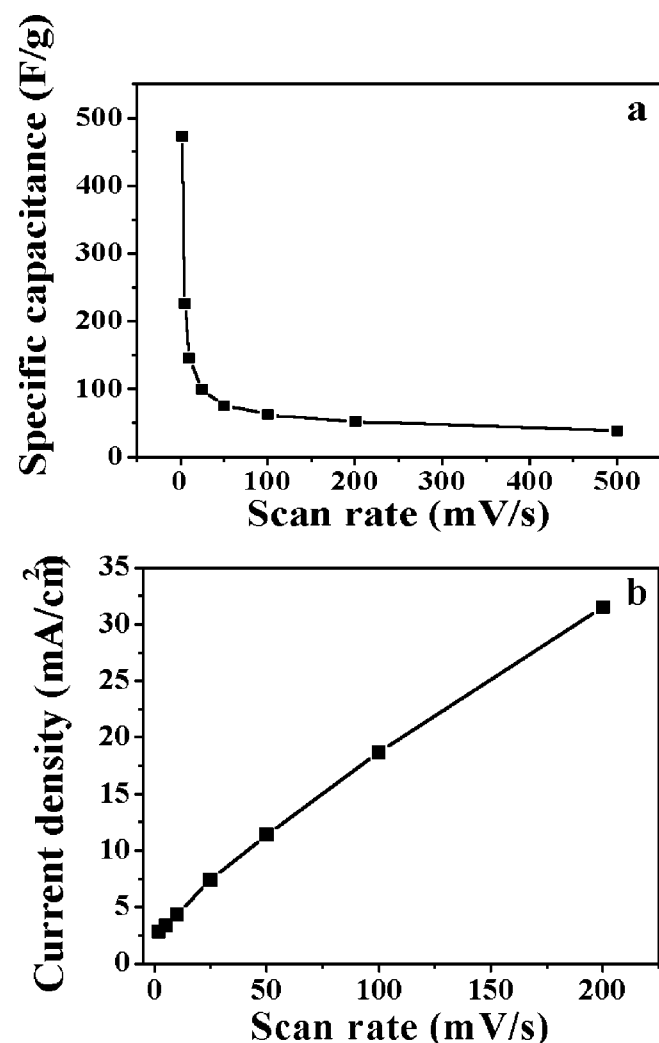


Figure 2. (a) Variation of specific capacitance of porous nickel electrode with different scan rates employed for the capacitance measurement using CV. (b) A plot of variation of current density vs. scan rate for the high surface area porous nickel obtained by template electrodeposition.

between -0.1 and $+0.2$ V vs. SCE. The limitation in potential window arises due to the redox reaction of nickel to nickel hydroxide at more positive potentials. A study involving nonaqueous electrolytes is underway to explore the possibility of extending the potential window.

EIS.—Nyquist plots of template deposited porous nickel electrode in 6 M KOH at two different dc potentials viz. -1.0 and -1.1 V vs. SCE are shown in Fig. 3a. It can be seen that the porous nickel electrode shows a high-frequency depressed semicircle (kinetic arc) and a low-frequency straight-line portion, in contrast to the depressed semicircle obtained for smooth nickel in the entire

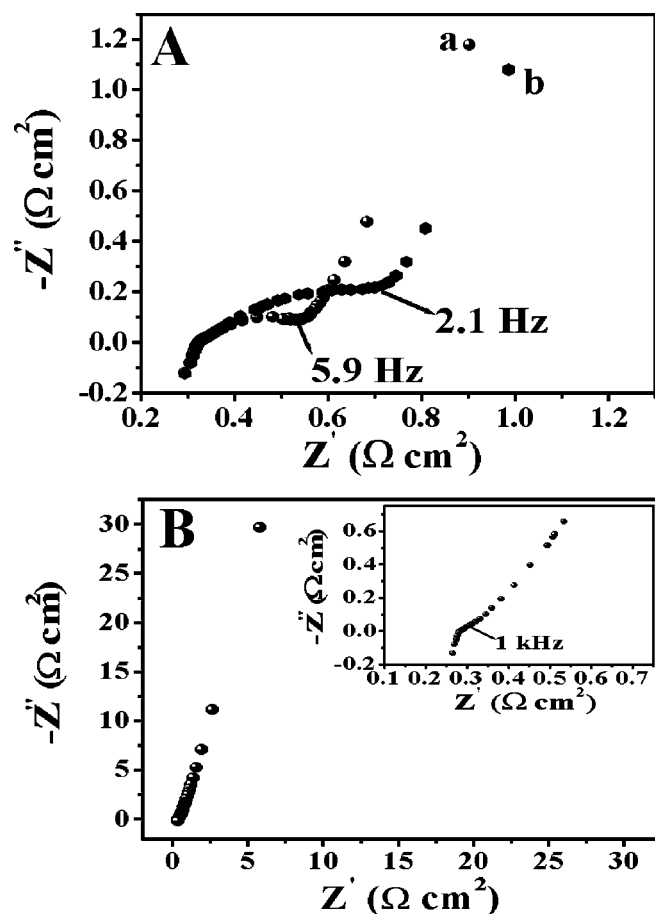
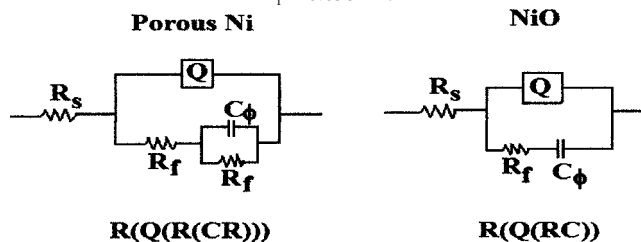


Figure 3. (A) Nyquist plots for the porous nickel electrode in 6 M KOH solution at two different dc potentials of (a) -1.1 and (b) -1.0 V vs. SCE. (B) Typical impedance (Nyquist) plot of the nickel oxide electrode in 6 M KOH solution. The inset shows the expanded high-frequency region of the same plot. Potential: 0 V vs. SCE.

Table II. Equivalent circuit fitting models and the parameters obtained using the fitting procedure for both the porous nickel and NiO electrodes.

Electrode	Porous nickel	Nickel oxide (NiO)
Equivalent circuit model	$R(Q(R(CR)))$	$R(Q(RC))$
Equivalent circuit fitting parameters	$R_s = 0.324 \Omega \text{ cm}^2$	$R_s = 0.29 \Omega \text{ cm}^2$
	$Q = 0.246$	$Q = 0.043$
	$n = 0.69$	$n = 0.82$
	$R_f = 0.658 \Omega \text{ cm}^2$	$R_f = 1.44 \Omega \text{ cm}^2$
	$C_\phi = 1.09 \text{ mF/cm}^2$	$C_\phi = 0.008 \text{ mF/cm}^2$
	$R_f = 0.658 \Omega \text{ cm}^2$	



range of frequencies used for the measurement (not shown). This behavior implies that the porous nickel electrode shows a blocking behavior at high frequency region and capacitive behavior with the phase angle close to 60° (not shown) at the low-frequency region. The impedance plots were fitted with appropriate equivalent circuits described by Conway for the electrochemical capacitors.³ The results of the fitting and the best-fit equivalent circuit for the impedance data at -1.0 V is shown in Table II. It can be seen that the model conforms to that described by Conway for the case of under potential deposition with continuous reaction.³ The pseudocapacitance (C_ϕ) contribution (1.09 mF/cm^2) due to the nickel hydride redox reaction is dominant at this potential while the double layer capacitance contribution is relatively less and cannot be computed due to the depressed nature of semicircle characteristic of porous electrodes. Figure 3b shows the Nyquist plots of nickel oxide electrode in 6 M KOH . A small semicircle at high frequencies (shown in the inset of figure) suggests that the reaction is charge transfer controlled at this region and a straight line with the phase angle of 80° at low frequency implies that the electrode can function as low leakage electrochemical capacitor in the double layer region. The impedance data for this system are fitted to several equivalent circuit models.³ The best fit equivalent circuit and the corresponding circuit elements are shown in the Table II. In contrast to the case of porous nickel electrode described earlier, the double layer capacitance component is dominant in the case of NiO electrode. However, a significant contribution from pseudocapacitance (C_ϕ) does arise due to OH^- adsorption on the electrode surface at this potential range.¹⁶

Complex capacitance and complex power analysis.—There have been several models proposed to explain the frequency behavior of supercapacitor materials such as transmission line model (TLM)³¹ and models based on size and shape of the pores (pore size distribution model).^{32,33} In our case, we have followed the simpler method of analysis of complex capacitance, $C(\omega)$ and complex power, $S(\omega)$.^{34,35} The complex power $S(\omega)$ contains the real part active power, $P(\omega)$ and the imaginary part reactive power $Q(\omega)$. Figures 4a and b present the plot of C'' vs. frequency for the template deposited porous nickel and nickel oxide electrodes respectively. The nickel oxide electrode shows a peak at f_0 while in the case of template deposited porous nickel electrode, the maximum has not been reached in the entire range of frequency used for the study.

Figures 5a and b show the normalized real part $|P|/|S|$ and the imaginary part $|Q|/|S|$ of the complex power vs. frequency (in logarithmic scale) for the porous nickel and nickel oxide electrodes respectively. At high frequency, when the supercapacitor behaves like

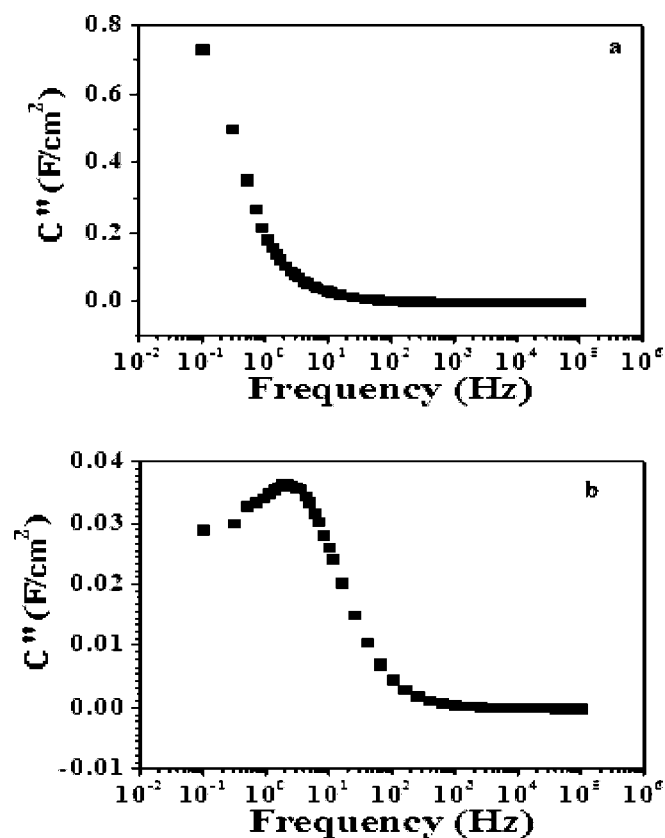


Figure 4. Plots of imaginary part of the complex capacitance vs. frequency for (a) the porous nickel and (b) the nickel oxide electrodes.

a pure resistance, all the power is dissipated into the system ($P = 100\%$) while no power is dissipated into a pure capacitance at low frequency. This can be seen from Fig. 5, where the value of $|P|/|S|$ decreases with decreasing frequency, while the normalized imaginary part of the complex power $|Q|/|S|$ increases with decreasing frequency. The maximum of $|Q|/|S|$ occurs at the low-frequency region where the supercapacitor behaves like a pure capacitance.

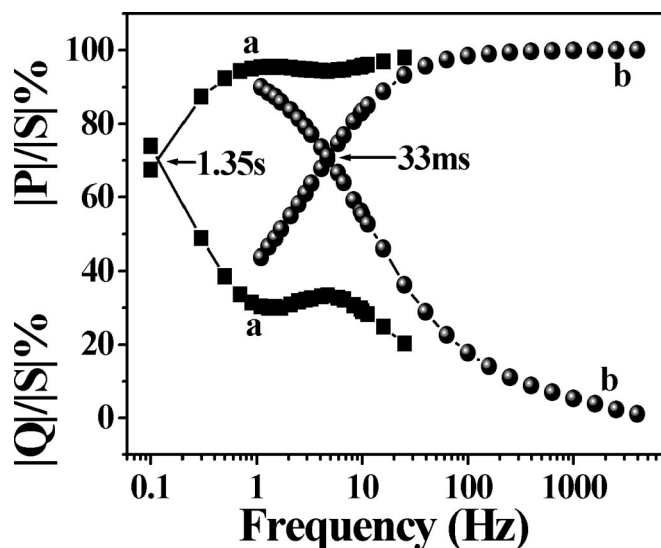


Figure 5. Plots of normalized reactive power $|Q|/|S|$ and active power $|P|/|S|$ vs. frequency for (a) the porous nickel and (b) the nickel oxide electrodes.

The time constant $\tau_o (=1/2 \pi f_o)$ determined at resonant frequency corresponds to the phase angle of 45° , which represents the transition for the electrochemical capacitor between a pure resistive (for $f > 1/\tau_o$) and a pure capacitive (for $f < 1/\tau_o$) behavior. From Fig. 5, τ_o values of 1.35 s and 33 ms were calculated for the porous nickel and nickel oxide (single electrodes), respectively, which implies fast power dissipation in the system. Low τ_o values are preferred in fast charging-discharging process and the values obtained in the present work imply that the material is quite fast in delivering energy with a higher power.

The analysis of the results shown in Fig. 4 and 5 indicate that the template deposited high surface area porous nickel has high energy density and the nickel oxide derived from it has a higher power density with faster response time. It is clear that the porous nickel as well as its corresponding nickel oxide electrodes are the promising sources of supercapacitor electrode materials. Using these results, a supercapacitor cell is being constructed and an evaluation of its performance as supercapacitor will be reported in due course.

Conclusions

We have studied the utility of the high surface area porous nickel obtained from the template electrodeposition and nickel oxide derived from it as electrochemical capacitor electrode materials. From the cyclic voltammetry studies of these electrodes in 6 M KOH, we measured a single electrode specific capacitance of 473 F/g for porous nickel electrode and 57 F/g for the NiO electrode. From the analysis of EIS data, we have determined a relaxation time constant of 1.35 s for the porous nickel and 33 ms for nickel oxide. These values suggest their utility in short time pulse devices that can deliver energy at a faster rate with much higher power. Our studies show that the material has excellent potential as an electrode in electrochemical capacitors. The work on the fabrication of devices based on the cell assembly of the porous nickel electrode is underway and will be reported elsewhere.

Acknowledgment

We thank Dr. N. G. Renganathan, CECRI, Karaikudi for many useful discussions. Help from the research colleagues in the laboratory at CECRI, Karaikudi is gratefully acknowledged.

The Raman Research Institute assisted in meeting the publication costs of this article.

References

1. V. Ganesh and V. Lakshminarayanan, *Electrochim. Acta*, **49**, 3561 (2004).
2. K. Kotz and M. Carlen, *Electrochim. Acta*, **45**, 2483 (2000).
3. B. E. Conway, *Electrochemical Supercapacitors: Scientific Fundamentals and Technological Applications*, Kluwer Academic/Plenum Publishers, New York (1999).
4. B. E. Conway, *J. Electrochem. Soc.*, **138**, 1539 (1991).
5. S. Sarangapani, B. V. Tilak, and C. P. Chen, *J. Electrochem. Soc.*, **143**, 3791 (1996).
6. A. J. Bard and L. R. Faulkner, *Electrochemical Methods: Fundamentals and Applications*, Wiley, New York (1980).
7. S. T. Mayer, R. W. Pekela, and J. L. Kaschmitter, *J. Electrochem. Soc.*, **140**, 446 (1993).
8. J. M. Miller, B. Dunn, T. D. Tran, and R. W. Pekela, *J. Electrochem. Soc.*, **144**, L309 (1997).
9. K. C. Liu and M. A. Anderson, *J. Electrochem. Soc.*, **143**, 124 (1996).
10. J. P. Zheng, P. J. Cygan, and T. R. Zow, *J. Electrochem. Soc.*, **142**, 2699 (1995).
11. B. E. Conway, in *Electrochemical Capacitors*, F. M. Delnick and M. Tomkiewicz, Editors, PV 95-29, p. 15, The Electrochemical Society Proceedings Series, Pennington, NJ (1995).
12. J. Kumaki, *Macromolecules*, **19**, 2258 (1986).
13. F. Henselwood and G. Liu, *Macromolecules*, **30**, 488 (1997).
14. K. C. Liu and M. A. Anderson, *J. Electrochem. Soc.*, **143**, 124 (1996).
15. V. Srinivasan and J. W. Weidner, *J. Electrochem. Soc.*, **144**, L210 (1997).
16. V. Srinivasan and J. W. Weidner, *J. Electrochem. Soc.*, **147**, 880 (2000).
17. E. E. Kalu, T. T. Nwoga, V. Srinivasan, and J. W. Weidner, *J. Power Sources*, **92**, 163 (2001).
18. C. Lin, J. A. Ritter, and B. N. Popov, *J. Electrochem. Soc.*, **145**, 4097 (1998).
19. S. C. Pang, M. A. Anderson, and T. W. Chapman, *J. Electrochem. Soc.*, **147**, 444 (2000).
20. P. A. Nelson and J. R. Owen, *J. Electrochem. Soc.*, **150**, A1313 (2003).
21. I. J. Brown and S. Sotiropoulos, *Electrochim. Acta*, **46**, 2711 (2001).
22. K. W. Nam and K. B. Kim, *J. Electrochem. Soc.*, **149**, A346 (2002).
23. K. W. Nam, W. S. Yoon, and K. B. Kim, *Electrochim. Acta*, **47**, 3201 (2002).
24. K. R. Prasad and N. Miura, *Electrochem. Commun.*, **6**, 849 (2004).
25. J. H. Chen, W. Z. Li, D. Z. Wang, S. X. Yang, J. G. Wen, and Z. F. Ren, *Carbon*, **40**, 1193 (2002).
26. V. Subramanian, S. C. Hall, P. H. Smith, and B. Rambabu, *Solid State Ionics*, **175**, 511 (2004).
27. K. R. Prasad and N. Miura, *Electrochem. Commun.*, **6**, 1004 (2004).
28. B. E. Conway, H. A. Kozłowska, M. A. Sattar, and B. V. Tilak, *J. Electrochem. Soc.*, **130**, 1825 (1983).
29. R. Juskenas, I. Valsiunas, V. Jasulaitiene, and V. Pakstas, *Electrochim. Acta*, **47**, 4239 (2002).
30. L. O. Valoen, S. Sunde, and R. Tunold, *J. Alloys Compd.*, **253**, 656 (1997).
31. D. Qu and H. Shi, *J. Power Sources*, **74**, 99 (1998).
32. H. K. Song, Y. H. Jung, K. H. Lee, and L. H. Dao, *Electrochim. Acta*, **44**, 3513 (1999).
33. H. Keiser, K. D. Beccu, and M. A. Gutjahr, *Electrochim. Acta*, **12**, 539 (1976).
34. P. L. Taberna, P. Simon, and J. F. Fauvarque, *J. Electrochem. Soc.*, **150**, A292 (2003).
35. E. Lust, A. Janes, and M. Arulepp, *J. Electroanal. Chem.*, **562**, 33 (2004).